
Robustness-Inspired Defense Against Backdoor Attacks on Graph Neural Networks

Zhiwei Zhang, Minhua Lin, Junjie Xu, Zongyu Wu, Enyan Dai, Suhang Wang
The Pennsylvania State University
{zbx5349, mfl5681, junjiexu, zongyuwu, emd5759, szw494}@psu.edu

Abstract

Graph Neural Networks (GNNs) have achieved promising results in tasks such as node classification and graph classification. However, recent studies reveal that GNNs are vulnerable to backdoor attacks, posing a significant threat to their real-world adoption. Despite initial efforts to defend against specific graph backdoor attacks, there is no work on defending against various types of backdoor attacks where generated triggers have different properties. Hence, we first empirically verify that prediction variance under edge dropping is a crucial indicator for identifying poisoned nodes. With this observation, we propose using random edge dropping to detect backdoors and theoretically show that it can efficiently distinguish poisoned nodes from clean ones. Furthermore, we introduce a novel robust training strategy to efficiently counteract the impact of the triggers. Extensive experiments on real-world datasets show that our framework can effectively identify poisoned nodes, significantly degrade the attack success rate, and maintain clean accuracy when defending against various types of graph backdoor attacks with different properties.

1 Introduction

Graphs are pervasive in real world such as social networks [1], molecular graphs [2], and knowledge graphs [3]. Graph Neural Networks (GNNs) have shown great ability in node representation learning on graphs. Generally, GNNs adopt a message-passing mechanism that updates a node’s representation by iteratively aggregating information from its neighbors. The resulting node representations retain both node attributes and local graph structure information, benefiting various downstream tasks such as node classification [4, 5, 6], graph classification [7], and link prediction [8].

Despite their great performance, recent studies [9, 10, 11, 12] show that GNNs are susceptible to backdoor attacks. Generally, backdoor attacks involve generating and attaching backdoor triggers to a small set of target nodes, which are then assigned a target class. These triggers can be predefined or created by a trigger generator and usually take the form of a node or subgraph. When a GNN model is trained on a backdoored dataset, it learns to associate the presence of the trigger with the target class. Consequently, during inference, the backdoored model will misclassify test nodes with the trigger attached as belonging to the target class, while still maintaining high accuracy on clean nodes without a trigger attached. Backdoor attacks on GNNs are particularly concerning due to their potential impact on critical real-world applications such as healthcare and financial services. For instance, in medical diagnosis networks, an attacker could embed backdoor triggers into the training data, leading the GNN model to misclassify certain medical conditions when the trigger is present.

Thus, graph backdoor attack and defense are attracting increasing attention and several initial efforts have been taken [10, 11, 12, 9]. For example, the seminal work SBA [11] adopts randomly generated graphs as triggers for graph backdoor attack. To improve the attack success rate, GTA [10] adopts a backdoor trigger generator to generate more powerful sample-specific triggers. Observing that

the backdoor trigger and target nodes tend to have low feature similarity, Dai et al. [9] propose a defense method called Prune, which removes edges that connect nodes with low cosine similarity. It significantly reduces the attack success rate (ASR) of previous works. To improve the stealthiness of backdoor attacks, they proposed unnoticeable backdoor attack method UGBA by maximizing the cosine similarity between backdoor triggers and target nodes. Zhang et. al., [12] show that backdoor triggers tend to be outliers which can be removed with graph outlier detection (OD). To address this, they further proposed DPGBA which can generate in-distribution triggers. Despite initial efforts on backdoor defense, they generally utilize backdoor specific properties to defend against specific backdoor and are ineffective across various types of backdoor triggers and attack methods.

Therefore, in this paper, we study an important problem of developing an effective graph backdoor defense method against various types of backdoor triggers and attack methods. In essence, we are faced with two challenges: **(i)** How to efficiently and precisely identify poisoned nodes and backdoor triggers, even when those triggers are indistinguishable from clean nodes? **(ii)** How to minimize the impact of backdoor triggers when some of the triggers are not identified? In an attempt to address these challenges, we propose a novel framework Robustness Inspired Graph Backdoor Defense (RIGBD). To efficiently and precisely identify poisoned nodes, we empirically show in Section 3.2 that removing edges linking backdoor triggers typically leads to large prediction variance for poisoned target nodes. Based on this observation, we propose training a backdoored model with specially designed graph convolution operations on a poisoned graph, performing random edge dropping, and identifying nodes with high prediction variance as poisoned nodes. With candidate poisoned nodes and identified target class, we propose a novel robust GNN training loss, which minimizes model’s prediction confidence on the target class for poisoned nodes to efficiently counteract the impact of the triggers. Such strategy is effective even if part of poisoned nodes are not identified in the training set.

Our **main contributions** are: **(i)** We empirically verify that poisoned nodes typically exhibit large prediction variance under edge dropping. **(ii)** Theoretical analysis guarantees that our specially designed graph convolution operations can precisely distinguish poisoned nodes from clean nodes through random edge dropping. **(iii)** We propose novel training strategy to train a backdoor robust GNN model even though some poisoned nodes are not identified. **(iv)** Extensive experiments show the effectiveness of RIGBD in defending against backdoor attacks and maintaining clean accuracy.

2 Related Work

Graph Backdoor Attacks. SBA [11] is a seminal work on graph backdoor attacks, which adopts randomly generated graphs as triggers. GTA [10] adopts a backdoor trigger generator to generate more powerful sample-specific triggers to improve the attack success rate. UGBA [9] introduces an unnoticeable loss function aimed at maximizing the cosine similarity between backdoor triggers and target nodes to improve the stealthiness of their attack. DPGBA [12] introduces an outlier detector and uses adversarial learning to generate in-distribution triggers, addressing low ASR or outlier issues in existing graph backdoor attacks. More about graph backdoor attacks are in Appendix A.

Graph Backdoor Defense. UGBA [9] denotes that the attributes of triggers differ significantly from the attached poisoned nodes in GTA [10], thereby violating the homophily property typically observed in real-world graphs. Thus they propose a defense method called Prune, which removes edges that connect nodes with low similarity. DPGBA [12] further indicates that although the triggers in UGBA [9] may demonstrate high similarity to target nodes, the triggers in both UGBA [9] and GTA [10] are still outliers. Thus they propose a defense method called OD, which involves training a graph auto-encoder and filtering out nodes with high reconstruction loss. More details about backdoor defense in non-structure data [13] and robust GNNs [14, 15, 16] are shown in Appendix A. Our work is inherently different from theirs: (i) we aim to defend against various types of graph backdoor attacks; (ii) we design a novel and theoretically guaranteed method to precisely identify poison nodes, aiming to degrade the attack success rate (ASR) without compromising clean accuracy.

3 Preliminary

3.1 Background and Problem Definition

We use $\mathcal{G} = (\mathcal{V}, \mathcal{E}, \mathbf{X})$ to denote an attributed graph, where $\mathcal{V} = \{v_1, \dots, v_N\}$ is the set of N nodes, $\mathcal{E} \subseteq \mathcal{V} \times \mathcal{V}$ is the set of edges, and $\mathbf{X} = \{\mathbf{x}_1, \dots, \mathbf{x}_N\}$ is the set of attributes of \mathcal{V} . $\mathbf{A} \in \mathbb{R}^{N \times N}$ is

the adjacency matrix of \mathcal{G} , where $\mathbf{A}_{ij} = 1$ if nodes v_i and v_j are connected; otherwise $\mathbf{A}_{ij} = 0$. In this paper, we focus on the inductive setting. Specifically, during the training stage, we are provided with a graph $\mathcal{G}_T = (\mathcal{V}_T, \mathcal{E}_T, \mathbf{X}_T)$. We use $\mathcal{V}_C \subseteq \mathcal{V}_T$ and $\mathcal{V}_B \subseteq \mathcal{V}_T$ to denote the clean node set and backdoored node set, respectively. A node $v_i \in \mathcal{V}_C$ is clean and labeled with the clean label y_i , whereas a node $v_j \in \mathcal{V}_B$ is backdoored and labeled with the target label y_t . The set $\mathcal{V}_T \setminus (\mathcal{V}_C \cup \mathcal{V}_B)$ denote the unlabeled nodes. The set of edges linking $v_i \in \mathcal{V}_B$ and the trigger g_i is denoted as $\mathcal{E}_B \in \mathcal{E}_T$. During the inference stage, we are given an unseen graph $\mathcal{G}_U = (\mathcal{V}_U, \mathcal{E}_U, \mathbf{X}_U)$ where $\mathcal{V}_U = \mathcal{V}_{UC} \cup \mathcal{V}_{UB}$. A node $v_i \in \mathcal{V}_{UC}$ is clean, while a node $v_j \in \mathcal{V}_{UB}$ is backdoored. Notably, \mathcal{G}_U is disjoint from the training graph \mathcal{G}_T , meaning $\mathcal{V}_U \cap \mathcal{V}_T = \emptyset$. The set of edges linking $v_j \in \mathcal{V}_{UB}$ and the trigger g_j is denoted by $\mathcal{E}_{UB} \in \mathcal{E}_U$. The neighbors of node v_i are denoted as $\mathcal{N}(i)$.

Threat Model. The attacker aims to add backdoor triggers, i.e., nodes or subgraphs, to a small set of target nodes \mathcal{V}_B in the training graph and label them as a target class y_t , so that a GNN trained on the poisoned graph will (i) memorize backdoor triggers and be misguided to classify nodes attached with triggers as y_t ; and (ii) behave normally for clean nodes without triggers attached. Specifically, given $\mathcal{V}_B \in \mathcal{V}$ as a set of target nodes, the attacker attaches the crafted triggers $g_i = (\mathbf{X}_i^g, \mathbf{A}_i^g)$ to the node $v_i \in \mathcal{V}_B$ and get poisoned node $\tilde{v}_i = a(v_i, g_i)$, where $a(\cdot)$ is the attachment operation. Then, the attacker assigns \mathcal{V}_B with target class y_t to form backdoored graph \mathcal{G}_T .

Defender’s Knowledge and Capability. During the training phase, the defender has access to the backdoored graph \mathcal{G}_T to train a classifier for node classification. However, the defender lacks information about which nodes belong to the backdoor node set \mathcal{V}_B and the target class y_t . During the inference phase, the defender is presented with an unseen backdoored graph \mathcal{G}_U for node classification.

Graph Backdoor Defense. With the above description, our defense problem is formally defined as: *Given a backdoored graph \mathcal{G}_T , we aim to train a backdoor-free GNN model f on \mathcal{G}_T so that it can defend against backdoor triggers during inference on an unseen backdoored graph \mathcal{G}_U , while maintaining accuracy on clean data. This is formally defined as $\min_f \sum_{v_i \in \mathcal{V}_{UC}} l(f(v_i), y_i) - \sum_{v_j \in \mathcal{V}_{UB}} l(f(\tilde{v}_j), y_t)$, where l is the classification loss.*

3.2 Prediction Variance Caused by Trigger Edge Dropping

Generally, graph backdoor attacks establish an edge between a trigger and a target node [10, 9, 11], which means the backdoor attack will fail if the edge linking the trigger and the target node is dropped. Furthermore, an explicit requirement for backdoor attacks is that the backdoored GNN model f_b behaves normally for clean nodes without triggers attached. Based on the analysis above, we make an *assumption*: given a backdoored graph \mathcal{G}_T , if the trigger edge $e_i \in \mathcal{E}_B$ linking the target node $v_i \in \mathcal{V}_B$ and trigger g_i is dropped, the prediction logits of the backdoored model for the poisoned target node v_i will typically change significantly, compared to the prediction change on the nodes connected by clean edges $e_j \in \mathcal{E}_T \setminus \mathcal{E}_B$ when these edges e_j are dropped.

To empirically verify our assumption, we conduct the following experiments: Given a backdoored graph, we first pretrain a backdoored model on this graph. For each node, we then iteratively drop each of its neighbors one by one and measure the prediction variance caused by dropping trigger edges \mathcal{E}_B and clean edges $\mathcal{E}_T \setminus \mathcal{E}_B$, respectively. We perform experiments on OGB-arxiv [17] with 565 triggers. The attack method is DPGBA [12]. The model architecture is a 2-layer GCN [5]. From the results shown in Fig. 1 (a), it is evident that dropping adversarial edge connecting backdoor trigger will result in a much larger prediction variance than dropping clean edges. More results on other datasets can be found in Appendix B.

Thus, an intuitive method for identifying a backdoor trigger or poisoned target node is to examine each edge individually. For instance, in a 2-layer GCN [5], we remove one of its neighbors at a time for each node and conduct inference based on the remaining 2-hop neighbors. By observing prediction changes with each neighbor removal, we estimate the likelihood of an edge being linked to the backdoor trigger: greater prediction change indicates a higher probability. However, this method has several issues: (i) *Scalability*: For graphs with high average degree, this method is computationally

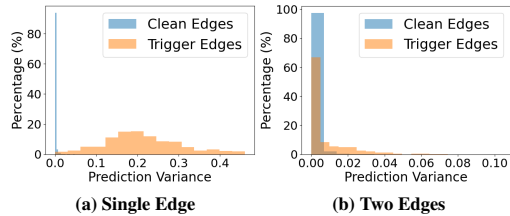


Figure 1: Prediction variance caused by dropping trigger edges and clean edges.

expensive. Specifically, for an L -layer GCN, the time complexity is $\mathcal{O}(LNd^LM(d+M))$, where d is the average degree, N is the number of nodes, and M denotes the feature dimension. The analysis is in Appendix C. As d grows, the time complexity grows exponentially with the power L , making it impractical for dense graphs. (ii) *Utility*: When the backdoor trigger is a subgraph with multiple edges linking it to a target node, examining each edge individually becomes ineffective. As shown in Fig. 1 (b), when two edges linking a trigger and a target node, on the OGB-arxiv dataset, most of the prediction variance caused by dropping trigger edges shows similar values to those caused by dropping clean edges, rendering the intuitive method ineffective.

Therefore, while prediction variance caused by edge dropping is a crucial indicator for identifying poisoned nodes or backdoor triggers, it is essential to develop a method that can (i) accurately identify poisoned nodes, even when multiple edges connect a trigger to a target node; and (ii) reduce the time complexity to scale linearly with the average degree, thereby improving scalability.

Vulnerability of Clean Model to Backdoor Triggers. Even if we can remove backdoor triggers from the training dataset, a graph backdoor trigger can still potentially lead to a successful attack as the attacker can craft a backdoor trigger that mimics the neighbor of nodes [12] from the target class. To verify this, we adopt the DPGBA [12] attack method and conduct experiments by removing the backdoor triggers from the training dataset. We then train a 2-layer GCN on this clean dataset and report the attack success rate (ASR) on the test dataset, as shown in Table 1. The Random ASR is calculated by $\frac{1}{C}$ as a reference, where C is the number of classes for each dataset. As shown in the table, even when the model is trained on a clean dataset, it can still react to a backdoor trigger that mimics the neighbor of nodes from the target class. Thus, simply removing the backdoor triggers from the training dataset is insufficient to defend against graph backdoor attacks.

	Cora	OGB-arxiv
Rand. ASR	14.29	2.5
ASR	34.72	5.4

4 Methodology

Our preliminary analysis shows that (1) removing adversarial edges linking triggers and poisoned target nodes typically results in higher prediction variance for poisoned target nodes; (2) simply removing backdoor triggers from the training dataset is insufficient to protect against backdoor triggers that mimic the distribution of neighboring nodes from the target class. To utilize the above information and solve our problem, we face two challenges: (1) How to devise an efficient method to find poisoned target nodes? (2) How to minimize the impact of backdoor triggers without degrading the clean accuracy? To address the above challenges, a novel framework RIGBD is proposed. Specifically, to address the first challenge, we theoretically and empirically verify that random edge dropping is an efficient way to distinguish the poisoned target nodes from clean nodes. To address the second challenge, we propose to minimize the prediction confidence of poisoned target nodes on the target class. This encourages the model to counteract the impact of the trigger. Next, we give the details of each component.

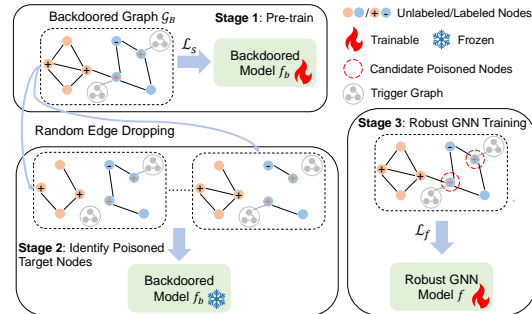


Figure 2: Framework of RIGBD

To address the above challenges, a novel framework RIGBD is proposed. Specifically, to address the first challenge, we theoretically and empirically verify that random edge dropping is an efficient way to distinguish the poisoned target nodes from clean nodes. To address the second challenge, we propose to minimize the prediction confidence of poisoned target nodes on the target class. This encourages the model to counteract the impact of the trigger. Next, we give the details of each component.

4.1 Identifying Poisoned Target Nodes by Random Edge Dropping

To overcome the scalability and utility issues of the intuitive method of dropping each edge individually, we propose a novel random edge dropping framework. Specifically, we define a randomized edge drop noise ϵ for adjacency matrix \mathbf{A} that removes each existing edge with the probability β as

$$P(\epsilon_{ij} = 0 \mid \mathbf{A}_{ij} = 0) = 1, P(\epsilon_{ij} = 1 \mid \mathbf{A}_{ij} = 1) = \beta, P(\epsilon_{ij} = 0 \mid \mathbf{A}_{ij} = 1) = 1 - \beta, \quad (1)$$

where $\epsilon_{ij} = 1$ means dropping edge e_{ij} . We denote $\mathbf{A} \oplus \epsilon$ as the perturbed graph, with \oplus the element-wise XOR operator. Given a backdoored graph \mathcal{G}_T and corresponding adjacency matrix \mathbf{A} , we first train the backdoored node classifier f_b on this poisoned graph \mathcal{G}_T and get the prediction logits \mathbf{p}_i for each node $v_i \in \mathcal{V}_L$, i.e., $\mathbf{p}_i = f_b(\mathbf{A}; v_i)$. Then, we independently add random noise

ϵ to the original adjacency matrix \mathbf{A} for K times using the operation $\mathbf{A} \oplus \epsilon$, resulting in the noisy matrices $\mathbf{A}_1, \dots, \mathbf{A}_K$. Similarly, we obtain the prediction logits $\mathbf{p}_i^k = f_b(\mathbf{A}_k; v_i)$ for node v_i on each perturbed graph. Then, the prediction variance of node v_i against random edge dropping is:

$$s(i) = \sum_{k=1}^K \text{KL}(\mathbf{p}_i, \mathbf{p}_i^k), \quad (2)$$

where $\text{KL}(\mathbf{p}_i, \mathbf{p}_i^k)$ denotes Kullback-Leibler divergence between \mathbf{p}_i and \mathbf{p}_i^k . With an appropriate K and β , it is highly likely that an edge connecting the backdoor trigger will be removed in one or more of the perturbed adjacency matrices, causing significant prediction variance for poisoned nodes.

However, it is unclear whether this method can also lead to large prediction variance for clean nodes, potentially compromising our ability to differentiate between poisoned target nodes and clean ones. To address this concern, we propose to obtain each node representation only based on its neighbors. Specifically, when performing inference to obtain the prediction logits \mathbf{p}_i and \mathbf{p}_i^k (before and after random edge dropping), the operation in each layer can be written as:

$$\mathbf{H}^{(l+1)} = \sigma \left(\tilde{\mathbf{D}}^{-\frac{1}{2}} \mathbf{A} \tilde{\mathbf{D}}^{-\frac{1}{2}} \mathbf{H}^{(l)} \mathbf{W}^{(l)} \right). \quad (3)$$

where \mathbf{A} is the adjacency matrix without self-connections. In contrast, GCN [5] obtain node representations by $\mathbf{H}^{(l+1)} = \sigma(\tilde{\mathbf{D}}^{-\frac{1}{2}}(\mathbf{A} + \mathbf{I})\tilde{\mathbf{D}}^{-\frac{1}{2}}\mathbf{H}^{(l)}\mathbf{W}^{(l)})$ where \mathbf{I} is the identity matrix.

We adopt the graph convolution strategy in Eq. (3) to get node representations for the following reasons: (1) For clean nodes, as each neighbor has the same drop ratio β , in expectation, the node representation is unchanged because the proportion of the expected contribution of each neighbor's features to the node representation is maintained. Thus, the expectation of prediction variance for clean nodes tends to be small. In contrast, if we include the attributes of the central node, the expectation of the node representation will focus more on the central node after random edge dropping, making the prediction variance unpredictable. We will analyze further in Theorem 1. (2) For poisoned target node, as backdoor triggers are designed to attack various types of targets, once the trigger exists after random edge dropping, it will still lead to a successful attack, regardless of whether the node representations are obtained only based on neighbors or also consider the node itself. However, if the trigger is dropped, the model will exhibit a large prediction variance. Notably, while the attributes of the central node are important for accurate classification, our focus here is on testing the prediction variance and identifying poisoned nodes. Once target nodes are identified, various GNNs can be used to train a classifier with our robust loss in Eq. (6).

To prove that our method of randomized edge dropping can effectively distinguish poisoned target nodes from clean nodes, we make the following assumptions on graph and propose theorems.

Assumptions on Graphs. Following [18, 19], we consider a graph \mathcal{G} , where each node v_i has features $\mathbf{x}_i \in \mathbb{R}^m$, a label y_i and $\text{deg}(i)$ denotes the number of its neighbors. We assume that: (1) The feature of node v_i is sampled from the feature distribution F_{y_i} that depends on the label y_i of the node, i.e., $\mathbf{x}_i \sim \mathcal{F}_{y_i}$. (2) Feature dimensions of \mathbf{x}_i are independent to each other; (3) The features in \mathbf{X} are bounded by a positive scalar B , i.e., $\max_{i,j} |\mathbf{X}[i,j]| \leq B$.

Theorem 1. Consider a graph $\mathcal{G} = \{\mathcal{V}, \mathcal{E}, \mathbf{X}\}$ following Assumptions (1)-(3). For clean node $v_i \in \mathcal{V}$ and its neighbors $\mathcal{N}(i)$, the expectation of the pre-activation output of a single operation defined in Eq. (3) is given by $\mathbb{E}[\mathbf{h}_i]$. Then the expectation of the pre-activation output of a single operation defined in Eq. (3) after random edge dropping is given by $\mathbb{E}[\mathbf{h}_i^k] = \mathbb{E}[\mathbf{h}_i]$.

The proof is in Appendix D.1. Theorem 1 shows that, in expectation, the output embedding of a node remains unchanged before and after random edge dropping when applying the layer operation defined in Eq. (3), regardless of the drop ratio. However, in practice, conducting numerous experiments is not feasible. Thus, we analyze the distance between the observed node embeddings after random edge dropping and the expectation of node embeddings without perturbation.

Theorem 2. Consider a graph $\mathcal{G} = \{\mathcal{V}, \mathcal{E}, \mathbf{X}\}$ following Assumptions (1)-(3). Let \mathbf{h}_i and \mathbf{h}_i^k denote the clean node embedding before and after the k -th random edge dropping, respectively, and $\text{deg}(i)_k$ represent the corresponding degree of node v_i . The probability that the distance between the observation \mathbf{h}_i^k and the expectation of \mathbf{h}_i is larger than t is bounded by:

$$\mathbb{P} \left(\left\| \mathbf{h}_i^k - \mathbb{E}[\mathbf{h}_i] \right\|_2 \geq t \right) \leq 2 \cdot M \cdot \exp \left(-\frac{\text{deg}(i)_k t^2}{2\rho^2(\mathbf{W})B^2M} \right), \quad (4)$$

where M denotes the feature dimension and $\rho^2(\mathbf{W})$ denotes the largest singular value of \mathbf{W} .

The proof is in Appendix D.2. Theorem 2 shows that the distance between the observed node embeddings after random edge dropping and the expectation of node embeddings without perturbation is small with a high probability. Furthermore, nodes with higher degrees are more likely to exhibit less variation in their embeddings. This highlights the effectiveness of our method of random edge dropping, particularly in dense graphs, compared to the method that drops each edge individually.

Based on the above analysis, we theoretically demonstrate that our method, which involves random edge dropping and obtaining node representations through graph convolution as defined in Eq. (3), results in small changes to node representations. Thus, for **clean nodes**, this stability ensures that the prediction output is consistent as the backdoored model does not exhibit sensitivity towards any particular clean neighbors. However, for **poisoned target nodes**, the scenario differs. Despite the stability in their node representations after random edge dropping, the last-layer classifier’s sensitivity [20] to the presence or absence of the backdoor trigger leads to a significant variance in prediction outcomes compared to clean nodes. This is verified in Sec. 3.2.

Next, we analyze the expected number of times the backdoor trigger g_i can be removed from the neighbor of a poisoned node v_i after K iterations of random edge dropping. This also indicates the expected number of times the poisoned node v_i demonstrates a larger prediction variance.

Theorem 3. *Without loss of generality, we consider the case where there is only one edge connecting a backdoor trigger to a target node. Let β denote the random edge dropping ratio, and K be the total number of iterations for random edge dropping and conducting inference on the perturbed graph. For a poisoned node v_i and a trigger g_i , the expected number of times the poisoned node v_i demonstrates large prediction variance is given as $\mathbb{E}(g_i)_d = K \cdot \beta$.*

Theorem 3 demonstrates that this expected number grows fast with a certain drop ratio. Since Theorem 1 indicates that, in expectation, the output embedding of a clean node remains unchanged before and after perturbation, regardless of the drop ratio, we can use a high drop ratio, e.g. $\beta = 0.5$, to achieve a fast increase in the expected number of times the poisoned node v_i demonstrates large prediction variance. Our experimental results in Section 5.4 show that with $\beta = 0.5$, even a small value of K , e.g. $K = 5$, can already identify most of the poisoned target nodes from the clean ones.

To empirically verify that our method of random edge dropping can efficiently distinguish poisoned nodes from clean nodes, we adopt the attack method DPGBA and conduct experiments on Cora and OGB-arxiv to show the prediction variance of poisoned nodes and clean nodes after random edge dropping. The details of the experiment settings and the results are in Appendix E. From the results, we observe that: **(i)** Our method consistently results in higher prediction variance for poisoned nodes, enabling the distinction between poisoned and clean nodes. **(ii)** Even when two edges link a backdoor trigger to a poisoned node, our method maintains high prediction variance for most poisoned nodes. This showcases the superior performance of our method compared to the intuitive approach of dropping each edge individually. Furthermore, the time complexity of our method scales linearly with K , which is typically small, whereas the intuitive method scales exponentially with d^L , leading to significantly higher computational costs as d increases.

Identify Target Nodes and Target Class. Next, we give details of how we determine the target class y_t and identify the candidate poisoned target node set \mathcal{V}_s . Given $s(i)$ as the prediction variance for each node $v_i \in \mathcal{V}_T$ with label y_i , we sort nodes by $s(i)$ in descending order and form the set $\mathcal{D}' = \{(s_{\sigma(1)}, y_{\sigma(1)}), (s_{\sigma(2)}, y_{\sigma(2)}), \dots, (s_{\sigma(n)}, y_{\sigma(n)})\}$, where σ is a permutation of $\{1, 2, \dots, n\}$ such that the sorted values satisfy $s_{\sigma(1)} > s_{\sigma(2)} > \dots > s_{\sigma(n)}$. Then we determine the target class as the label of the node with the largest prediction variance, i.e., $y_t = y_{\sigma(1)}$. Let j be the index of the first entry in \mathcal{D}' such that $y_{\sigma(j)} \neq y_t$ and $y_{\sigma(j+1)} \neq y_t$. The threshold of prediction variance to select candidate poisoned target nodes is defined as:

$$\tau = s_{\sigma(j)} \quad \text{where} \quad j = \min \{k \mid y_{\sigma(k)} \neq y_t \text{ and } y_{\sigma(k+1)} \neq y_t, k = 1, 2, 3, \dots, n\}. \quad (5)$$

Then, we select nodes with prediction variance larger than the threshold τ as candidates for poisoned target nodes, denoted as \mathcal{V}_s .

4.2 Backdoor Robust GNN Model Training

Though random edge dropping can help identify the most poisoned target nodes, there are still some concerns. *First*, a small amount of poisoned target nodes might exhibit prediction variances similar to those of clean nodes, inevitably remaining within the graph. *Second*, as discussed in Section 3.2,

merely eliminating backdoor triggers from the training set is insufficient to defend against backdoor triggers that mimic the neighbor distribution of nodes from the target class.

An intuitive solution is to train a trigger detector capable of distinguishing clean nodes and backdoor triggers. Then, during inference on an unseen graph \mathcal{G}_U , the trigger detector is adopted to remove potential triggers. However, when the trigger is a subgraph, multiple nodes, and their interactions need to be considered simultaneously during training, complicating the process of training the trigger detector. Additionally, each time we are given an unseen graph, we need to run the trigger generator to perform inference on the entire graph first, increasing the computational cost.

Thus, in our RIGBD, we propose directly training a backdoor robust GNN node classifier f on the training dataset \mathcal{V}_L by minimizing its prediction confidence on the target class y_t for poisoned nodes, thereby encouraging the model to counteract the impact of the backdoor triggers and be robust against backdoor attack. Specifically, given the selected poisoned target nodes $\mathcal{V}_s \in \mathcal{V}_T$, the objective function to train a backdoor robust GNN node classifier f is:

$$\min_f \mathcal{L}_f = \sum_{v_i \in \mathcal{V}_s} \log f(v_i)_{y_t} + \sum_{v_j \in \mathcal{V}_L \setminus \mathcal{V}_s} \mathcal{L}(f(v_j), y_j), \quad (6)$$

where $f(v_i)_{y_t}$ denotes the prediction confidence of f for v_i on target class y_t and $\mathcal{L}(f(v_j), y_j)$ is the cross entropy loss. The resulting classifier is robust against triggers as (i) We explicitly countermeasure the detected backdoors, making our model robust to backdoor. Though there might be target nodes not detected, they generally have smaller prediction variance, meaning that they have less impact on the training of f . As these triggers more or less have patterns similar to the detected ones, our training strategy implicitly mitigates their effects. (ii) For triggers that mimic the neighbor distribution of nodes from the target class, our model f is encouraged to explore the subtle differences between clean nodes from the target class and poisoned target nodes, thereby ensuring its clean accuracy. The training algorithm is in Appendix F.

5 Experiments

In this section, we conduct experiments to answer the following research questions: **(Q1)** How effective is RIGBD in defending against graph backdoor attacks? **(Q2)** How is the performance of RIGBD in detecting poisoned nodes? **(Q3)** How do different drop ratios and different numbers of iterations of random edge dropping impact the performance of RIGBD?

5.1 Experimental Setup

Datasets. We conduct experiments on three benchmark datasets widely used for node classification, i.e., Cora, Pubmed [21], and OGB-arxiv [17]. Cora and Pubmed are small citation networks. OGB-arxiv is a large-scale citation network. More details of the datasets are summarized in Appendix G.1.

Attack Methods. To demonstrate the defense ability of our RIGBD, we evaluate RIGBD on 3 state-of-the-art graph backdoor attack methods, i.e. GTA [10], UGBA [9] and DPGBA [12]. The details of these attacks are given in Appendix G.2.

Compared Methods. We implement the backdoor defense strategies Prune [9] and OD [12]. Additionally, three representative robust GNNs, i.e. RobustGCN [15], GNNGuard [14] and randomized smoothing (RS) [16] with various drop ratios are also selected. We also include ABL [13], which is a popular backdoor defense method in the image domain and aims to train clean models given backdoor-poisoned data. More details of these defense methods are given in Appendix G.3.

Evaluation Protocol. Following existing representative graph backdoor attacks [9, 12], we conduct experiments on the inductive node classification task. Specifically, we split the graph into two disjoint subgraphs, \mathcal{G}_T and \mathcal{G}_U , with an 80 : 20 ratio. The graph \mathcal{G}_T is used to train the attacker. Then, the attacker selects target nodes \mathcal{V}_B and attaches triggers to these target nodes to form the backdoored graph \mathcal{G}_T . The number of triggers $|\mathcal{V}_B|$ is set as 40, 160, and 565 for Cora, PubMed, and OGB-arxiv, respectively. The trigger size is limited to three nodes in all experiments. The defender trains a model on poisoned graph \mathcal{G}_T . Next, half of the nodes in \mathcal{G}_U are selected as poisoned nodes and are attached with backdoor triggers to test the attack success rate (ASR). The remaining nodes in \mathcal{G}_U are kept clean and used to test the clean accuracy (ACC). We also report the Recall and Precision of our method in identifying poisoned nodes. Recall is defined as the percentage of poisoned nodes among the candidate nodes identified, relative to all poisoned nodes. Precision is defined as the percentage

Table 2: Results of backdoor defense.

Attacks	Defense	Cora		PubMed		OGB-arxiv	
		ASR(%) ↓	ACC(%) ↑	ASR(%) ↓	ACC(%) ↑	ASR(%) ↓	ACC(%) ↑
GTA	GCN	98.98	82.58	93.09	85.18	75.34	65.76
	GNNGuard	40.22	78.52	26.93	81.68	0.04	62.58
	RobustGCN	90.46	80.37	93.12	81.68	70.95	56.08
	Prune	17.63	83.06	28.10	85.05	0.01	63.97
	OD	0.04	83.47	0.03	85.27	0.01	65.23
	RS	53.14	73.33	42.28	84.58	42.72	58.48
	ABL	19.93	81.85	16.18	83.92	11.28	63.24
	RIGBD	0.00	83.70	0.01	84.32	0.01	66.51
UGBA	GCN	98.76	83.42	96.42	84.64	98.82	63.95
	GNNGuard	43.17	78.15	98.97	81.48	95.21	64.61
	RobustGCN	98.67	80.00	99.90	82.85	90.35	56.18
	Prune	98.89	82.66	92.87	85.09	93.07	62.58
	OD	0.03	83.65	0.01	85.19	0.01	65.35
	RS	54.24	70.37	44.41	84.68	40.30	58.76
	ABL	15.13	81.48	28.60	84.37	34.26	64.93
	RIGBD	0.01	84.81	0.01	85.13	0.01	66.21
DPGBA	GCN	97.72	83.34	98.63	85.22	95.63	65.72
	GNNGuard	85.61	78.52	44.12	80.82	94.66	62.29
	RobustGCN	96.68	81.11	94.88	82.54	90.09	60.38
	Prune	91.82	85.28	88.64	85.13	90.47	65.53
	OD	94.33	83.58	91.32	85.12	93.30	65.47
	RS	51.29	69.63	48.83	85.44	41.18	58.44
	ABL	86.72	79.26	48.58	79.45	52.56	63.88
	RIGBD	0.01	85.19	0.01	84.32	0.00	65.24

of poisoned nodes among the candidate nodes identified. Our RIGBD deploys a 2-layer GCN as the model architecture. Each experiment is conducted 5 times and the average results are reported.

5.2 Performance of Defense

To answer **Q1**, we compare RIGBD with the baseline defense methods across three datasets. The number of iterations for random edge dropping is set to $K = 20$, with a drop ratio of $\beta = 0.5$. We report ASR and ACC in Table 2. From the table, we observe: **(i)** Across all datasets and attack methods, RIGBD consistently achieves the lowest ASR score, typically close to 0%. Although defense methods such as Prune and OD perform well against GTA and UGBA attacks, they fail to defend against DPGBA, which generates in-distribution triggers. This indicates that RIGBD is highly effective in defending against various types of backdoor triggers and backdoor attacks. **(ii)** Our RIGBD achieves comparable or slightly better clean accuracy compared to the vanilla GCN. This indicates that our approach of random edge dropping typically leads to higher prediction variance for poisoned nodes, effectively identifying backdoor triggers. In cooperation with this precise identification of poisoned nodes, our strategy to train a backdoor robust model using Eq. (6) can significantly reduce the ASR while maintaining clean accuracy. Additional results on RS with varying drop ratios and RIGBD using different GNN architectures can be found in Appendix I.

5.3 Ability to Detect Poisoned Nodes

To answer **Q2**, we present the recall and precision of RIGBD in identifying poisoned nodes. Using the same setting as in Sec. 5.2, the results on OGB-arxiv are shown in Table 3. We also include

Table 3: Results for the ability to detect poisoned nodes.

Attacks	Clean ACC	ASR	ACC	Recall	Precision
GTA	65.8	0.01	66.51	84.9	90.3
UGBA	65.8	0.01	65.21	95.6	96.3
DPGBA	65.8	0.00	65.24	90.5	93.9

the corresponding ASR and ACC to illustrate the correlation between detection ability and defense performance. Clean accuracy (Clean ACC), obtained from a model trained on the clean graph, is provided as a reference to evaluate the model’s performance on clean nodes. From the table, we observe the following: **(i)** Our RIGBD demonstrates consistently high precision, always over 90%, in detecting poisoned nodes across three attack methods, with detection recall always exceeding 80%. This indicates that our strategy of random edge dropping typically leads to higher prediction variance for poisoned nodes. **(ii)** Although the recall for the GTA attack method is 84.9%, we still achieve an ASR close to 0% while maintaining ACC. This verifies the stability of our strategy to train a robust node classifier using Eq. (6). Even when some poisoned nodes are still identified, it still efficiently helps the model unlearn the triggers. More results on other datasets are in Appendix J.

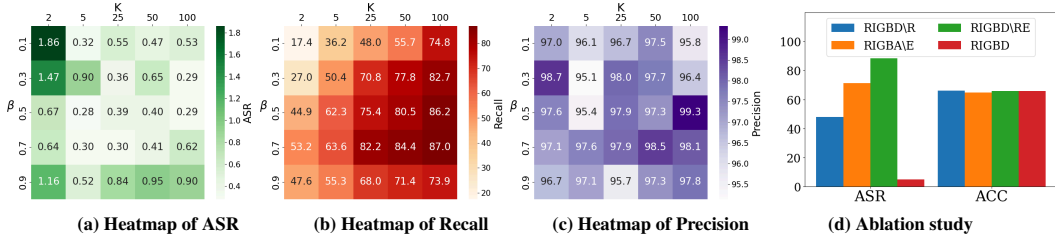


Figure 3: Hyperparameter Sensitivity Analysis and Ablation Study.

5.4 Hyperparameter Analysis and Ablation Study

Hyperparameter Analysis. To answer **Q3**, we conduct experiments to show how different drop ratios β and different numbers of iterations of random edge dropping K impact the performance of RIGBD. Specifically, we vary the value of K as $\{2, 5, 25, 50, 100\}$, and the values of β as $\{0.1, 0.3, 0.5, 0.7, 0.9\}$. The attack method used is DPGBA. The other settings are the same as the evaluation protocol in Sec. 5.1. The results on OGB-*arxiv* are shown in Fig. 3. From the figure, we observe: (i) Our RIGBD is stable in terms of ASR and Precision. Notably, when the drop ratio $\beta = 0.1$ and $K = 2$, the recall of poisoned node detection is around 17.4%. However, we still achieve robust defense performance with 1.86% ASR. This is because our framework identifies the most efficient triggers that lead to large prediction variance and focuses on minimizing their impact. By doing so, the influence of less efficient triggers is inherently counteracted. In contrast, when we simply remove those 17.4% triggers from the dataset and train a normal GNN on the remaining dataset, the ASR is around 80%. (ii) As K increases, the recall also increases, empirically verifying our theorems that the clean nodes will have stable node embeddings and predictions. As β increases from 0.1 to 0.7, the recall also increases without a decrease in precision. When $\beta = 0.9$, only about 10% of edges remain in each iteration. Although the recall decreases slightly, we still achieve consistently high precision. This further shows the robustness of RIGBD against various chosen hyperparameters. More results on the hyperparameter analysis for ACC are in Appendix K.

Ablation Study. To evaluate the effectiveness of random edge dropping, we replace it with the intuitive method of dropping edges individually, as described in Section 3.2, and obtain a variant named as RIGBD\AE. We then conduct experiments focusing on scenarios where a backdoor trigger (subgraph) is linked to a poisoned node by two edges. To demonstrate the effectiveness of our robust training strategy, we implement a variant of our model, named RIGBD\R, which simply removes identified candidate poisoned nodes from the dataset and trains a GNN classifier with cross-entropy. We also implement a variant called RIGBD\RE, which involves individually dropping each edge and eliminating candidate poisoned nodes. The number of iterations for random edge dropping is set to $K = 20$, with a drop ratio of $\beta = 0.5$. The attack method used is DPGBA. The dataset is OGB-*arxiv*. We report the ASR and ACC in Fig. 3. From the figure, we observe: (i) When two edges link a backdoor trigger to a target node, the intuitive method of dropping each edge individually fails to defend against this attack. Notably, RIGBD\R achieves an ASR almost 40% lower than RIGBD\AE, highlighting that our random edge dropping is more efficient than dropping edges individually in identifying poisoned nodes. (ii) In cooperation with a robust training strategy, our RIGBD further achieves an ASR close to 0%. This underscores the superiority of our method in defending against various types of backdoor attacks. Additional results on the ablation study for the case where one edge links a trigger and a target node can be found in Appendix L.

Performance Under Different Number of Triggers. The performance and analysis of RIGBD against different attack budgets is provided in the Appendix M.

6 Conclusion

In this paper, we first empirically show that poisoned nodes exhibit high prediction variance with edge dropping. We then propose random edge dropping, supported by theoretical analysis, to efficiently and precisely identify poisoned nodes. Additionally, we introduce a robust training strategy to develop a backdoor-robust GNN model, even if some poisoned nodes remain unidentified. Extensive experiments demonstrate that our method accurately detects poisoned nodes, significantly reduces the attack success rate, and maintains clean accuracy against various graph backdoor attacks.

References

- [1] Wenqi Fan, Yao Ma, Qing Li, Yuan He, Eric Zhao, Jiliang Tang, and Dawei Yin. Graph neural networks for social recommendation. In *The world wide web conference*, pages 417–426, 2019.
- [2] Elman Mansimov, Omar Mahmood, Seokho Kang, and Kyunghyun Cho. Molecular geometry prediction using a deep generative graph neural network. *Scientific reports*, 9(1):20381, 2019.
- [3] Zhiwei Liu, Liangwei Yang, Ziwei Fan, Hao Peng, and Philip S Yu. Federated social recommendation with graph neural network. *ACM Transactions on Intelligent Systems and Technology (TIST)*, 13(4):1–24, 2022.
- [4] Will Hamilton, Zhitao Ying, and Jure Leskovec. Inductive representation learning on large graphs. *Advances in neural information processing systems*, 30, 2017.
- [5] Thomas N Kipf and Max Welling. Semi-supervised classification with graph convolutional networks. *arXiv preprint arXiv:1609.02907*, 2016.
- [6] Petar Velickovic, Guillem Cucurull, Arantxa Casanova, Adriana Romero, Pietro Lio, Yoshua Bengio, et al. Graph attention networks. *stat*, 1050(20):10–48550, 2017.
- [7] Keyulu Xu, Weihua Hu, Jure Leskovec, and Stefanie Jegelka. How powerful are graph neural networks? *arXiv preprint arXiv:1810.00826*, 2018.
- [8] Muhan Zhang and Yixin Chen. Link prediction based on graph neural networks. *Advances in neural information processing systems*, 31, 2018.
- [9] Enyan Dai, Minhua Lin, Xiang Zhang, and Suhang Wang. Unnoticeable backdoor attacks on graph neural networks. In *Proceedings of the ACM Web Conference 2023, WWW '23*. ACM, April 2023.
- [10] Zhaohan Xi, Ren Pang, Shouling Ji, and Ting Wang. Graph backdoor. In *30th USENIX Security Symposium (USENIX Security 21)*, pages 1523–1540, 2021.
- [11] Zaixi Zhang, Jinyuan Jia, Binghui Wang, and Neil Zhenqiang Gong. Backdoor attacks to graph neural networks. In *Proceedings of the 26th ACM Symposium on Access Control Models and Technologies*, pages 15–26, 2021.
- [12] Zhiwei Zhang, Minhua Lin, Enyan Dai, and Suhang Wang. Rethinking graph backdoor attacks: A distribution-preserving perspective. In *30th SIGKDD Conference on Knowledge Discovery and Data Mining*, 2024.
- [13] Yige Li, Xixiang Lyu, Nodens Koren, Lingjuan Lyu, Bo Li, and Xingjun Ma. Anti-backdoor learning: Training clean models on poisoned data. *Advances in Neural Information Processing Systems*, 34:14900–14912, 2021.
- [14] Xiang Zhang and Marinka Zitnik. Gnn-guard: Defending graph neural networks against adversarial attacks. *Advances in neural information processing systems*, 33:9263–9275, 2020.
- [15] Dingyuan Zhu, Ziwei Zhang, Peng Cui, and Wenwu Zhu. Robust graph convolutional networks against adversarial attacks. In *Proceedings of the 25th ACM SIGKDD International Conference on Knowledge Discovery & Data Mining*, pages 1399–1407, 2019.
- [16] Binghui Wang, Jinyuan Jia, Xiaoyu Cao, and Neil Zhenqiang Gong. Certified robustness of graph neural networks against adversarial structural perturbation. In *Proceedings of the 27th ACM SIGKDD Conference on Knowledge Discovery & Data Mining*, pages 1645–1653, 2021.
- [17] Weihua Hu, Matthias Fey, Marinka Zitnik, Yuxiao Dong, Hongyu Ren, Bowen Liu, Michele Catasta, and Jure Leskovec. Open graph benchmark: Datasets for machine learning on graphs. In H. Larochelle, M. Ranzato, R. Hadsell, M.F. Balcan, and H. Lin, editors, *Advances in Neural Information Processing Systems*, volume 33, pages 22118–22133. Curran Associates, Inc., 2020.
- [18] Enyan Dai, Shijie Zhou, Zhimeng Guo, and Suhang Wang. Label-wise graph convolutional network for heterophilic graphs. In *Learning on Graphs Conference*, pages 26–1. PMLR, 2022.
- [19] Yao Ma, Xiaorui Liu, Neil Shah, and Jiliang Tang. Is homophily a necessity for graph neural networks? *arXiv preprint arXiv:2106.06134*, 2021.
- [20] Bryant Chen, Wilka Carvalho, Nathalie Baracaldo, Heiko Ludwig, Benjamin Edwards, Taesung Lee, Ian Molloy, and Biplav Srivastava. Detecting backdoor attacks on deep neural networks by activation clustering. *arXiv preprint arXiv:1811.03728*, 2018.

- [21] Prithviraj Sen, Galileo Namata, Mustafa Bilgic, Lise Getoor, Brian Galligher, and Tina Eliassi-Rad. Collective classification in network data. *AI Magazine*, 29(3):93, Sep. 2008.
- [22] Yiming Li, Yong Jiang, Zhifeng Li, and Shu-Tao Xia. Backdoor learning: A survey. *IEEE Transactions on Neural Networks and Learning Systems*, 2022.
- [23] Tianyu Gu, Kang Liu, Brendan Dolan-Gavitt, and Siddharth Garg. Badnets: Evaluating backdooring attacks on deep neural networks. *IEEE Access*, 7:47230–47244, 2019.
- [24] Xinyun Chen, Chang Liu, Bo Li, Kimberly Lu, and Dawn Song. Targeted backdoor attacks on deep learning systems using data poisoning. *arXiv preprint arXiv:1712.05526*, 2017.
- [25] Hong Sun, Ziqiang Li, Pengfei Xia, Heng Li, Beihao Xia, Yi Wu, and Bin Li. Efficient backdoor attacks for deep neural networks in real-world scenarios. *arXiv preprint arXiv:2306.08386*, 2023.
- [26] Changjiang Li, Ren Pang, Zhaohan Xi, Tianyu Du, Shouling Ji, Yuan Yao, and Ting Wang. An embarrassingly simple backdoor attack on self-supervised learning. In *Proceedings of the IEEE/CVF International Conference on Computer Vision*, pages 4367–4378, 2023.
- [27] Yunfei Liu, Xingjun Ma, James Bailey, and Feng Lu. Reflection backdoor: A natural backdoor attack on deep neural networks. In *Computer Vision—ECCV 2020: 16th European Conference, Glasgow, UK, August 23–28, 2020, Proceedings, Part X 16*, pages 182–199. Springer, 2020.
- [28] Yuezun Li, Yiming Li, Baoyuan Wu, Longkang Li, Ran He, and Siwei Lyu. Invisible backdoor attack with sample-specific triggers. In *Proceedings of the IEEE/CVF international conference on computer vision*, pages 16463–16472, 2021.
- [29] Khoa Doan, Yingjie Lao, and Ping Li. Backdoor attack with imperceptible input and latent modification. In M. Ranzato, A. Beygelzimer, Y. Dauphin, P.S. Liang, and J. Wortman Vaughan, editors, *Advances in Neural Information Processing Systems*, volume 34, pages 18944–18957. Curran Associates, Inc., 2021.
- [30] Keita Kurita, Paul Michel, and Graham Neubig. Weight poisoning attacks on pre-trained models. *arXiv preprint arXiv:2004.06660*, 2020.
- [31] Huili Chen, Cheng Fu, Jishen Zhao, and Farinaz Koushanfar. Proflip: Targeted trojan attack with progressive bit flips. In *Proceedings of the IEEE/CVF International Conference on Computer Vision*, pages 7718–7727, 2021.
- [32] Ruixiang Tang, Mengnan Du, Ninghao Liu, Fan Yang, and Xia Hu. An embarrassingly simple approach for trojan attack in deep neural networks. In *Proceedings of the 26th ACM SIGKDD international conference on knowledge discovery & data mining*, pages 218–228, 2020.
- [33] Bolun Wang, Yuanshun Yao, Shawn Shan, Huiying Li, Bimal Viswanath, Haitao Zheng, and Ben Y Zhao. Neural cleanse: Identifying and mitigating backdoor attacks in neural networks. In *2019 IEEE Symposium on Security and Privacy (SP)*, pages 707–723. IEEE, 2019.
- [34] Soheil Kolouri, Aniruddha Saha, Hamed Pirsiavash, and Heiko Hoffmann. Universal litmus patterns: Revealing backdoor attacks in cnns. In *Proceedings of the IEEE/CVF Conference on Computer Vision and Pattern Recognition*, pages 301–310, 2020.
- [35] Binghui Wang, Xiaoyu Cao, Neil Zhenqiang Gong, et al. On certifying robustness against backdoor attacks via randomized smoothing. *arXiv preprint arXiv:2002.11750*, 2020.
- [36] Maurice Weber, Xiaojun Xu, Bojan Karlaš, Ce Zhang, and Bo Li. Rab: Provable robustness against backdoor attacks. In *2023 IEEE Symposium on Security and Privacy (SP)*, pages 1311–1328. IEEE, 2023.
- [37] Chulin Xie, Minghao Chen, Pin-Yu Chen, and Bo Li. Crfl: Certifiably robust federated learning against backdoor attacks. In *International Conference on Machine Learning*, pages 11372–11382. PMLR, 2021.
- [38] Derrick Blakely, Jack Lanchantin, and Yanjun Qi. Time and space complexity of graph convolutional networks. *Accessed on: Dec, 31:2021*, 2021.

A Details of Related Works

A.1 Graph Backdoor Attacks

Backdoor attacks have been extensively studied in the image domain [22, 23, 24, 25, 26]. Initial works focused on directly poisoning training samples [27, 24], while others explored making the triggers invisible [28, 29]. Additionally, hidden backdoors can be embedded through transfer learning [30], modifying model parameters [31], and adding extra malicious modules [32]. Recently, studies have begun investigating backdoor attacks on GNNs, which differ from the more common poisoning and evasion attacks. Backdoor attacks involve injecting malicious triggers into the training data, causing the model to make incorrect predictions when these triggers are present in test samples. This type of attack subtly manipulates the training phase, ensuring the model performs as expected under normal conditions but fails when trigger-embedded inputs are present. Among pioneering efforts, SBA [11] introduced a method for injecting universal triggers into training samples using a subgraph-based approach, though its attack success rate was low. GTA [10] advanced this by developing a technique for generating adaptive triggers, customizing perturbations for individual samples to enhance attack effectiveness. In UGBA [9], an algorithm for selecting poisoned nodes was introduced to optimize the attack budget, along with an adaptive trigger generator to create triggers with high cosine similarity to the target node. DPGBA [12] demonstrate that existing backdoor attack methods on graphs suffer from either a low attack success rate or outlier issues. To address these problems, they propose an adversarial learning strategy to generate in-distribution triggers and introduce a novel loss function to enhance the attack success rate with these in-distribution triggers.

A.2 Graph Backdoor Defense

Backdoor defenses have been extensively investigated in the context of non-structured data. To address the threat of backdoor attacks, various defenses have been proposed, which can be broadly classified into two main categories: empirical backdoor defenses and certified backdoor defenses. Empirical backdoor defenses [33, 34, 13] are based on specific observations or understandings of existing attacks and generally perform well in practice; however, they lack theoretical guarantees and may be circumvented by adaptive attacks. On the other hand, certified backdoor defenses [35, 36, 37] offer theoretical guarantees of their validity under certain assumptions, but their practical performance is often weaker than empirical defenses due to the difficulty in meeting these assumptions. Improving defenses against backdoor attacks remains a significant open challenge. Limited defenses have been proposed against the graph backdoor. UGBA [9] highlights that in attack methods GTA [10], the attributes of triggers differ significantly from the attached poisoned nodes, violating the homophily property typically observed in real-world graphs. To address this, they propose a defense method called Prune, which involves removing edges that connect nodes with low cosine similarity. This approach significantly reduces ASR of previous works. DPGBA [12] further notes that although the generated triggers in UGBA [9] may demonstrate high cosine similarity to target nodes, the triggers in both UGBA [9] and GTA [10] are still outliers. Thus, they propose a defense method called OD, which involves training a graph auto-encoder and filtering out nodes with high reconstruction loss. Their empirical results show that existing backdoor attack methods on graphs suffer from either a low ASR or outlier issues. However, there is no existing work on defending against DPGBA, which generates in-distribution triggers.

B Additional Empirical Results on Prediction Variance Caused by Edge Dropping

In this section, we show additional results on prediction variance caused by dropping trigger edges and clean edges on Cora and PubMed datasets. We generate 40 triggers for Cora and 160 triggers for PubMed. The attack method used is DPGBA [12]. The model architecture is a 2-layer GCN [5]. The results are shown in Fig. 4. From the figure, it is evident that dropping adversarial edge connecting backdoor trigger will typically result in a much larger prediction variance than dropping clean edges.

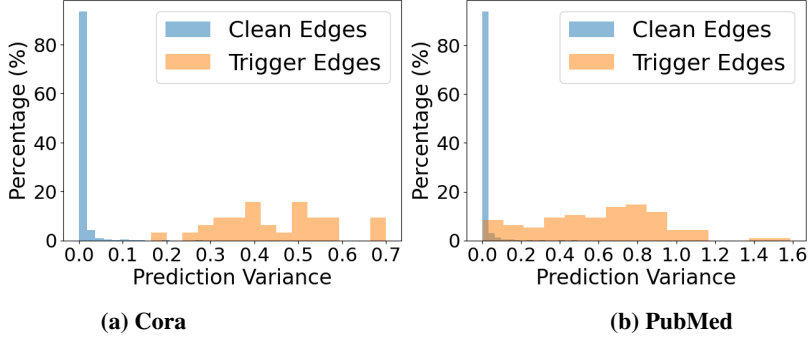


Figure 4: Visualization of prediction variance caused by dropping trigger edges and clean edges.

C Time Complexity Analysis

Following [38], to show the computation of a GCN, first we define $\hat{\mathbf{A}} = \mathbf{A} + \mathbf{I}$, the adjacency matrix with self-loops. $\hat{\mathbf{D}}$ is the diagonal degree matrix of $\hat{\mathbf{A}}$. \mathbf{A}' is the normalized adjacency matrix given as:

$$\mathbf{A}' = \hat{\mathbf{D}}^{-\frac{1}{2}} \hat{\mathbf{A}} \hat{\mathbf{D}}^{-\frac{1}{2}} \quad (7)$$

The computation of the l -th layer of a GCN network is:

$$\mathbf{X}^{(l+1)} = \sigma(\mathbf{A}' \mathbf{X}^{(l)} \mathbf{W}^{(l)}) \quad (8)$$

where $\sigma(\cdot)$ is a non-linear activation function (typically ReLU) and $\mathbf{W}^{(l)}$ is a feature transformation matrix $\in \mathbb{R}^{M_l \times M_{l+1}}$.

Thus, we analyze the complexity of the forward step by decomposing Equation (8) into three high-level operations:

1. $\mathbf{Z}^{(l)} = \mathbf{X}^{(l)} \mathbf{W}^{(l)}$: feature transformation
2. $\mathbf{X}^{(l+1)} = \mathbf{A}' \mathbf{Z}^{(l)}$: neighborhood aggregation
3. $\sigma(\cdot)$: activation

Part 1 is a dense matrix multiplication between matrices of size $N \times M_l$ and $M_l \times M_{l+1}$. We assume for all l , $M_l = M_{l+1} = M$. Therefore, this is $\mathcal{O}(NM^2)$.

Naively, part 2 involves multiplying matrices of sizes $N \times N$ and $N \times M$, resulting in a time complexity of $\mathcal{O}(N^2M)$. However, in practice, we use a sparse operator like PyTorch's `scatter` function to compute this. For each row (i, j) of the edge matrix \mathbf{E} , we compute $\mathbf{x}_i^{(l+1)} += \mathbf{z}_j^{(l)}$, where $\mathbf{x}_i^{(l+1)}$ and $\mathbf{z}_j^{(l)}$ are M -dimensional vectors. This results in a total cost of $\mathcal{O}(|E|M)$, where $|E|$ is the total number of edges. Alternatively, considering each node has d neighbors on average, neighborhood aggregation for each node requires $\mathcal{O}(dM)$, leading to a total cost of $\mathcal{O}(NdM) = \mathcal{O}(|E|M)$.

Part 3 is simply an element-wise function, so its cost is $\mathcal{O}(N)$.

Over L layers, this results in time complexity $\mathcal{O}(L(NM^2 + NdM + N)) = \mathcal{O}(L(NM^2 + NdM)) = \mathcal{O}(L(NM^2 + |E|M))$. Next, we ignore the time complexity of activation for simplicity in our analysis.

Random edge dropping: For random edge dropping and conduct inference on the whole graph for K times. The overall time complexity over L layers is $\mathcal{O}(LK(NM^2 + |E|M))$.

Dropping each edge individually: For each node, we drop one of its neighbors and conduct inference on its L -hop subgraph centered at the node using an L -layer GNN, we repeat this process for d times. For simplicity, we assume each node has d -neighbors. Thus, an L -hop subgraph has in total $\mathcal{O}(d^L)$ nodes. The time complexity analysis for each node is as follows. We use the L -hop subgraph as input to the L -layer GNN. In each GNN layer: (1) For feature transformation, the time complexity is $\mathcal{O}(d^L M^2)$. (2) For each neighbor aggregation, the time complexity is $\mathcal{O}(d^L M)$. As we conduct d times aggregation, the time complexity is $\mathcal{O}(d^{L+1} M)$. Thus, over N nodes and L -layer, the time complexity is $\mathcal{O}(LN d^L M (d + M))$.

As d^L is usually much larger than K in practice, the intuitive method is inefficient due to the high computational cost. We conduct empirical experiments to compare the running time on the OGB-arxiv dataset. We use the same experimental setup as described in Section 5.2. The results are shown in Tab. 4. We set $K = 10$ for RIGBD. From the table, we observe that RIGBD is significantly more efficient compared to the intuitive method in empirical experiments.

Table 4: Running Time Comparison

Intuitive	RIGBD ($K = 10$)
42.56s	0.09s

D Detailed Proofs

Assumptions on Graphs. Following [18, 19], we consider a graph \mathcal{G} , where each node v_i has features $\mathbf{x}_i \in \mathbb{R}^m$, a label y_i and $\text{deg}(i)$ denotes the number of its neighbors. We assume that: (1) The feature of node v_i is sampled from the feature distribution F_{y_i} that depends on the label y_i of the node, i.e., $\mathbf{x}_i \sim \mathcal{F}_{y_i}$. This means that the feature of the node is influenced by its label, with $\mu(\mathcal{F}_{y_i})$ denoting the mean of the distribution. (2) Feature dimensions of \mathbf{x}_i are independent to each other; (3) The features in \mathbf{X} are bounded by a positive scalar B , i.e., $\max_{i,j} |\mathbf{X}[i, j]| \leq B$;

These assumptions are reasonable in the context of graph machine learning for several reasons: Feature Distribution Based on Labels (Assumption 1): In many real-world scenarios, the features of a node are influenced by its label. For example, in a social network, the attributes of a user (like interests or activities) are often correlated with their group or community (label). Independence of Feature Dimensions (Assumption 2): In many datasets, especially high-dimensional ones, the correlations between features may be weak or negligible. Bounded Features (Assumption 3): In real-world datasets, feature values are often bounded due to physical, biological, or other practical constraints. Furthermore, in practice, features are often normalized or standardized during preprocessing, effectively bounding them within a certain range.

D.1 Proof of Theorem 1

Theorem 1. Consider a graph $\mathcal{G} = \{\mathcal{V}, \mathcal{E}, \mathbf{X}\}$ following Assumptions (1)-(3). For clean node $v_i \in \mathcal{V}$ and its neighbors $\mathcal{N}(i)$, the expectation of the pre-activation output of a single operation defined in Eq. (3) is given by $\mathbb{E}[\mathbf{h}_i]$. Then the expectation of the pre-activation output of a single operation defined in Eq. (3) after random edge dropping is given by $\mathbb{E}[\mathbf{h}_i^k] = \mathbb{E}[\mathbf{h}_i]$.

Proof. Given the graph convolution operation defined in Eq. (3), we obtain node representation $\mathbb{E}[\mathbf{h}_i] = \mathbb{E} \left[\sum_{j \in \mathcal{N}(i)} \frac{1}{\sqrt{\text{deg}(i)}\sqrt{\text{deg}(j)}} \mathbf{W} \mathbf{x}_j \right]$ For any node $v_i \in \mathcal{V}$ and its neighbors $\mathcal{N}(i)$, after random edge dropping with drop ratio β , in expectation, each neighbor in $\mathcal{N}(i)$ contributes with a weight of $(1 - \beta)$, and the expected $\text{deg}(i)$ is also scaled by $(1 - \beta)$. Therefore, the expectation of the pre-activation output of a single operation defined in Eq. (3) after random edge dropping is given by

$$\begin{aligned} \mathbb{E}[\mathbf{h}_i^k] &= \mathbb{E} \left[\sum_{j \in \mathcal{N}(i)} \frac{1}{\sqrt{(1 - \beta)\text{deg}(i)}\sqrt{(1 - \beta)\text{deg}(j)}} \mathbf{W}(1 - \beta)\mathbf{x}_j \right] \\ &= \mathbb{E} \left[\sum_{j \in \mathcal{N}(i)} \frac{1}{(1 - \beta)\sqrt{\text{deg}(i)}\sqrt{\text{deg}(j)}} \mathbf{W}(1 - \beta)\mathbf{x}_j \right] = \mathbb{E}[\mathbf{h}_i], \end{aligned} \tag{9}$$

which completes the proof. \square

D.2 Proof of Theorem 2

To prove Theorem 2, we first introduce the celebrated Hoeffding inequality.

Lemma 1. (Hoeffding's Inequality). Let Z_1, \dots, Z_n be independent bounded random variables with $Z_i \in [a, b]$ for all i , where $-\infty < a \leq b < \infty$. Then

$$\mathbb{P} \left(\frac{1}{n} \sum_{i=1}^n (Z_i - \mathbb{E}[Z_i]) \geq t \right) \leq \exp \left(-\frac{2nt^2}{(b-a)^2} \right)$$

and

$$\mathbb{P} \left(\frac{1}{n} \sum_{i=1}^n (Z_i - \mathbb{E}[Z_i]) \leq -t \right) \leq \exp \left(-\frac{2nt^2}{(b-a)^2} \right)$$

for all $t \geq 0$.

Theorem 2. Consider a graph $\mathcal{G} = \{\mathcal{V}, \mathcal{E}, \mathbf{X}\}$ following Assumptions (1)-(3). Let \mathbf{h}_i and \mathbf{h}_i^k denote the clean node embedding before and after the k -th random edge dropping, respectively, and $\deg(i)_k$ represent the corresponding number of remaining neighbors. The probability that the distance between the observation \mathbf{h}_i^k and the expectation of \mathbf{h}_i is larger than t is bounded by:

$$\mathbb{P} \left(\left\| \mathbf{h}_i^k - \mathbb{E}[\mathbf{h}_i] \right\|_2 \geq t \right) \leq 2 \cdot M \cdot \exp \left(-\frac{\deg(i)_k t^2}{2\rho^2(\mathbf{W})B^2M} \right), \quad (10)$$

where M denotes the feature dimensionality and $\rho^2(\mathbf{W})$ denotes the largest singular value of \mathbf{W} .

Proof. Following [18, 19], we consider a d -regular graph \mathcal{G} , i.e. each node has d neighbors, then the expectation of \mathbf{h}_i can be derived as $\mathbb{E}[\mathbf{h}_i] = \mathbb{E} \left[\sum_{j \in \mathcal{N}(i)} \frac{1}{\deg(i)} \mathbf{W} \mathbf{x}_j \right]$. Let $\mathbf{x}_j^k[m], n = 1, \dots, M$ denote the m -th element of \mathbf{x}_j^k . Then, for any dimension m , $\{\mathbf{x}_j^k[m], j \in \mathcal{N}(i)\}$ is a set of independent random variables bounded by $[-B, B]$. Hence, directly applying Hoeffding's inequality, for any $t_1 \geq 0$, we have the following bound:

$$\mathbb{P} \left(\left| \frac{1}{\mathcal{N}(i)^k} \sum_{j \in \mathcal{N}(i)^k} (\mathbf{x}_j^k[m] - \mathbb{E}[\mathbf{x}_j^k[m]]) \right| \geq t_1 \right) \leq 2 \exp \left(-\frac{(\deg(i)_k)t_1^2}{2B^2} \right) \quad (11)$$

if $\left\| \frac{1}{\mathcal{N}(i)^k} \sum_{j \in \mathcal{N}(i)^k} (\mathbf{x}_j^k - \mathbb{E}[\mathbf{x}_j^k]) \right\|_2 \geq \sqrt{M}t_1$, then at least for $m \in \{1, \dots, M\}$, the inequality $\left| \frac{1}{\mathcal{N}(i)^k} \sum_{j \in \mathcal{N}(i)^k} (\mathbf{x}_j^k[m] - \mathbb{E}[\mathbf{x}_j^k[m]]) \right| \geq t_1$ holds. Hence, we have

$$\begin{aligned} \mathbb{P} \left(\left\| \frac{1}{\mathcal{N}(i)^k} \sum_{j \in \mathcal{N}(i)^k} (\mathbf{x}_j - \mathbb{E}[\mathbf{x}_j]) \right\|_2 \geq \sqrt{M}t_1 \right) &\leq \mathbb{P} \left(\bigcup_{m=1}^M \left\{ \left| \frac{1}{\mathcal{N}(i)^k} \sum_{j \in \mathcal{N}(i)^k} (\mathbf{x}_j^k[m] - \mathbb{E}[\mathbf{x}_j^k[m]]) \right| \geq t_1 \right\} \right) \\ &\leq \sum_{m=1}^M \mathbb{P} \left(\left| \frac{1}{\mathcal{N}(i)^k} \sum_{j \in \mathcal{N}(i)^k} (\mathbf{x}_j^k[m] - \mathbb{E}[\mathbf{x}_j^k[m]]) \right| \geq t_1 \right) \\ &= 2 \cdot l \cdot \exp \left(-\frac{(\deg(i)_k)t_1^2}{2B^2} \right) \end{aligned} \quad (12)$$

Let $t_1 = \frac{t_2}{\sqrt{M}}$, then we have

$$\mathbb{P} \left(\left\| \frac{1}{\mathcal{N}(i)^k} \sum_{j \in \mathcal{N}(i)^k} (\mathbf{x}_j - \mathbb{E}[\mathbf{x}_j]) \right\|_2 \geq t_2 \right) \leq 2 \cdot M \cdot \exp \left(-\frac{(\deg(i)_k)t_1^2}{2B^2M} \right) \quad (13)$$

Furthermore, we have

$$\begin{aligned} \left\| \mathbf{h}_i^k - \mathbb{E}[\mathbf{h}_i^k] \right\|_2 &= \left\| \mathbf{W} \left(\frac{1}{\mathcal{N}(i)^k} \sum_{j \in \mathcal{N}(i)^k} (\mathbf{x}_j^k - \mathbb{E}[\mathbf{x}_j^k]) \right) \right\|_2 \\ &\leq \|\mathbf{W}\|_2 \left\| \frac{1}{\mathcal{N}(i)^k} \sum_{j \in \mathcal{N}(i)^k} (\mathbf{x}_j^k - \mathbb{E}[\mathbf{x}_j^k]) \right\|_2 \\ &= \rho(\mathbf{W}) \left\| \frac{1}{\mathcal{N}(i)^k} \sum_{j \in \mathcal{N}(i)^k} (\mathbf{x}_j^k - \mathbb{E}[\mathbf{x}_j^k]) \right\|_2, \end{aligned} \quad (14)$$

where $\|\mathbf{W}\|_2$ is the matrix 2-norm of \mathbf{W} . We denote $\rho(\mathbf{W}) = \|\mathbf{W}\|_2$. Given $\mathbb{E}[\mathbf{h}_i] = \mathbb{E}[\mathbf{h}_i^k]$, we have

$$\begin{aligned}
\mathbb{P}(\|\mathbf{h}_i^k - \mathbb{E}[\mathbf{h}_i]\|_2 \geq t) &= \mathbb{P}(\|\mathbf{h}_i^k - \mathbb{E}[\mathbf{h}_i^k]\|_2 \geq t) \\
&\leq \mathbb{P}\left(\rho(\mathbf{W}) \left\| \frac{1}{\mathcal{N}(i)^k} \sum_{j \in \mathcal{N}(i)^k} (\mathbf{x}_j^k - \mathbb{E}[\mathbf{x}_j^k]) \right\|_2 \geq t\right) \\
&= \mathbb{P}\left(\left\| \frac{1}{\mathcal{N}(i)^k} \sum_{j \in \mathcal{N}(i)^k} (\mathbf{x}_j^k - \mathbb{E}[\mathbf{x}_j^k]) \right\|_2 \geq \frac{t}{\rho(\mathbf{W})}\right) \\
&\leq 2 \cdot M \cdot \exp\left(-\frac{\deg(i)_k t^2}{2\rho^2(\mathbf{W})B^2M}\right),
\end{aligned} \tag{15}$$

which completes the proof. \square

D.3 Proof of Theorem 3

Theorem 3. *Without loss of generality, we consider the case where there is only one edge connecting a backdoor trigger to a target node. Let β denote the random edge dropping ratio, and K be the total number of iterations for random edge dropping and conducting inference on the perturbed graph. For a poisoned node v_i and a trigger g_i , the expected number of times the poisoned node v_i demonstrates large prediction variance is given as $\mathbb{E}(g_i)_d = K \cdot \beta$.*

Proof. We model the random edge-dropping process as a series of independent Bernoulli trials. Each trial represents a single iteration of edge-dropping, with a success probability β , which is the probability that the edge connecting v_i and g_i is dropped in that iteration.

Let X_k be an indicator random variable for the k -th iteration, where $X_k = 1$ if the edge is dropped, and $X_k = 0$ otherwise. The total number of times the edge is dropped over K iterations is then the sum of these indicator variables:

$$X = \sum_{k=1}^K X_k \tag{16}$$

Since each X_k follows a Bernoulli distribution with parameter β , the sum X follows a Binomial distribution with parameters K and β :

$$X \sim \text{Binomial}(K, \beta) \tag{17}$$

The expected value of a Binomial distribution is given by the product of the number of trials and the success probability. Therefore, the expected number of times the poisoned node v_i shows large prediction variance is:

$$E(g_i)_d = K \times \beta, \tag{18}$$

which completes the proof. \square

E Empirical Results of Prediction Variance for Different Attacks and Datasets using Random Edge Dropping

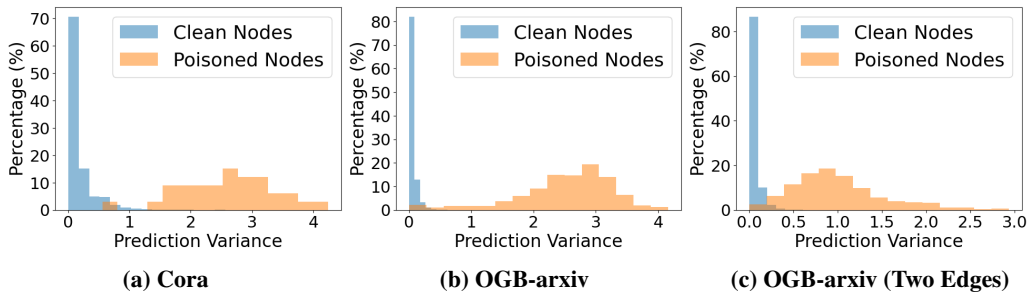


Figure 5: Visualization of prediction variance caused by random edge dropping.

To empirically verify that our method of random edge dropping can efficiently distinguish poisoned nodes from clean nodes, we conduct experiments on the Cora [21], PubMed, and OGB-arxiv [17] datasets, using 40 triggers for Cora, 160 triggers for PubMed and 565 triggers for OGB-arxiv, respectively. The attack method used is DPGBA [12]. The model architecture is a 2-layer GCN [5]. We set the drop ratio $\beta = 0.5$ and performed $K = 10$ iterations of random edge dropping. The results are shown in Fig. 5. In Figs. 5(a) and (b), we show the results for Cora and OGB-arxiv, respectively. In Fig. 5(c), we show the result for OGB-arxiv with two edges linking a backdoor trigger and a target node. Our observations are as follows: **(i)** Our method consistently results in higher prediction variance for poisoned nodes, thus enabling the distinction between poisoned nodes and clean nodes. **(ii)** Even when two edges link a backdoor trigger to a poisoned node, our method still results in high prediction variance for most of the poisoned nodes. This demonstrates the superior performance of our method compared to the intuitive approach of dropping each edge individually. Additional visualizations of prediction variance under different attacks on various datasets are in Fig. 6, Fig. 7 and Fig 8.

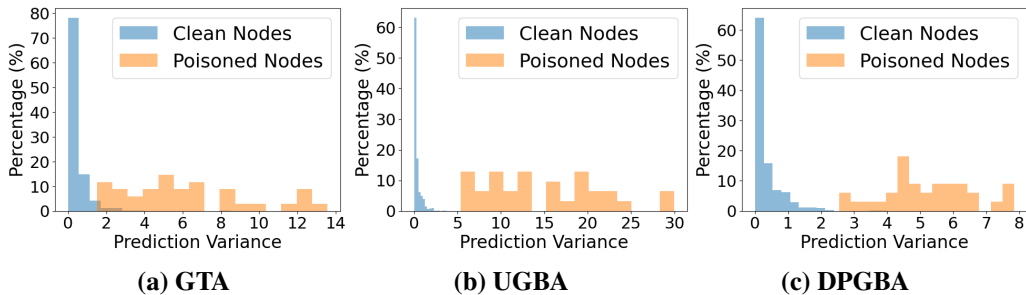


Figure 6: Visualization of prediction variance caused by random edge dropping on Cora dataset, drop ratio $\beta = 0.5$, drop iterations $K = 20$ and the number of triggers is 40.

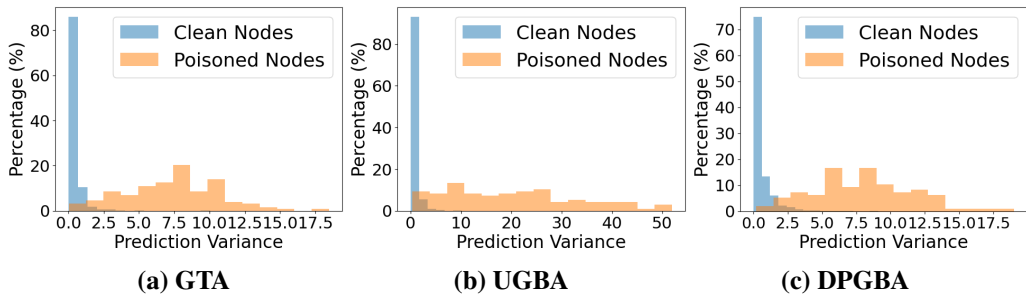


Figure 7: Visualization of prediction variance caused by random edge dropping on PubMed dataset, drop ratio $\beta = 0.5$, drop iterations $K = 20$ and the number of triggers is 160.

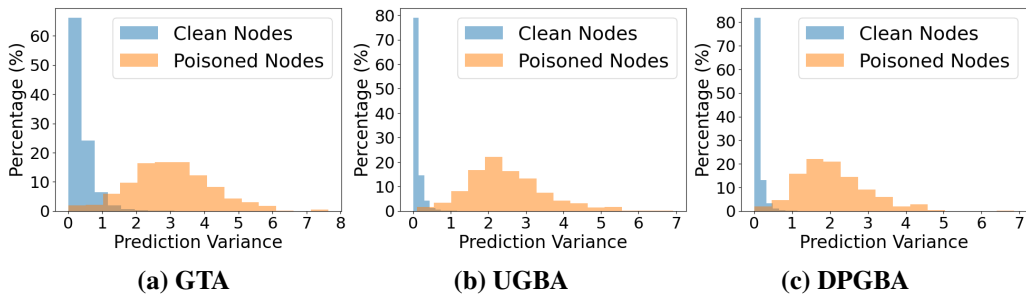


Figure 8: Visualization of prediction variance caused by random edge dropping on OGB-arxiv dataset, drop ratio $\beta = 0.5$, drop iterations $K = 20$ and the number of triggers is 565.

F Training Algorithm

We summarize the training method of RIGBD for training a backdoor robust GNN node classifier in Algorithm 1. Specifically, we start by randomly initializing the parameters θ_b for an L-layer GNN node classifier f_b , which uses the graph convolution operation defined in Eq. (3) (line 1). In each iteration of the training loop (lines 2-4), we update θ_b by training f_b on the backdoored graph \mathcal{G}_T by training f_b on the backdoored graph \mathcal{G}_T using supervised learning until the model converges. After convergence, we enter a second loop (lines 5-8) where we conduct random edge dropping on \mathcal{G}_T and perform inference with the backdoor model f_b (line 6). For each node, we calculate the prediction variance $s(i)$ using Eq. (2) (line 7). Nodes with prediction variance $s(i) > \tau$ are selected as candidate poisoned nodes \mathcal{V}_s , where τ is calculated by Eq. (5). Next, we randomly initialize θ for another L-layer GNN node classifier f (line 10). In the final training loop (lines 11-13), we update θ by training f using the robust training strategy defined in Eq. (6) until convergence. The algorithm concludes by returning the backdoor robust GNN node classifier f (line 14).

Algorithm 1 Algorithm of RIGBD

Require: Backdoored graph $\mathcal{G}_T = (\mathcal{V}_T, \mathcal{E}_T, \mathbf{X}_T)$, drop ratio β and number of drop iterations K

Ensure: Backdoor robust node classifier f

- 1: Randomly initialize θ_b for a L -layer GNN node classifier f_b with graph convolution operation defined in Eq. (3);
 - 2: **while** not converged yet **do**
 - 3: Update θ_b by training f_b on the backdoored graph \mathcal{G}_T using supervised learning;
 - 4: **end while**
 - 5: **for** $k = 1, 2, \dots, K$ **do**
 - 6: Conduct random edge dropping on the graph \mathcal{G}_T and perform inference with the backdoor model f_b ;
 - 7: Calculate the prediction variance $s(i)$ for each node by Eq. (2);
 - 8: **end for**
 - 9: Select candidate poisoned nodes \mathcal{V}_s for nodes with prediction variance $s(i) > \tau$, where τ is calculated by Eq. (5).
 - 10: Randomly initialize θ for any L -layer GNN node classifier f ;
 - 11: **while** not converged yet **do**
 - 12: Update θ by training f using the robust training strategy defined in Eq. (6);
 - 13: **end while**
 - 14: **return** Backdoor robust GNN node classifier f ;
-

G Additional Details of Experiment Settings

G.1 Dataset Statistics

Cora and PubMed are citation networks where nodes denote papers, and edges depict citation relationships. In Cora, each node is described using a binary word vector, indicating the presence or absence of a corresponding word from a predefined dictionary. In contrast, PubMed employs a TF/IDF weighted word vector for each node. For both datasets, nodes are categorized based on their respective research areas. OGB-arxiv is a citation network encompassing all Computer Science arXiv papers cataloged in the Microsoft Academic Graph. Each node is characterized by a 128-dimensional feature vector, which is derived by averaging the skip-gram word embeddings present in its title and abstract. Additionally, the nodes are categorized based on their respective research areas. The statistics details of these datasets are summarized in Table 5.

Table 5: Dataset Statistics

Datasets	#Nodes	#Edges	#Features	#Classes
Cora	2,708	5,429	1,443	7
Pubmed	19,717	44,338	500	3
OGB-arxiv	169,343	1,166,243	128	40

G.2 Attack Methods

The details of attack methods are described following:

1. **GTA** [10]: GTA utilizes a trigger generator that crafts subgraphs as triggers tailored to individual samples. The optimization of the trigger generator focuses exclusively on the backdoor attack loss, disregarding any constraints related to trigger detectability.
2. **UGBA** [9]: UGBA selects representative and diverse nodes as poisoned nodes to fully utilize the attack budget. An adaptive trigger generator is optimized with a constraint loss so that the generated triggers are ensured to be similar to the target nodes.
3. **DPGBA** [9]: DPGBA introduce adversarial learning strategy to generate in-distribution triggers. A novel loss is proposed to help adaptive trigger generator to generate efficient in-distribution triggers.

G.3 Compared Methods

We select two defense methods that aim to defend against specific backdoor attack methods:

1. **Prune** [9]: Prune is designed to prune edges that linking nodes with low similarity to remove those triggers that are totally different from clean nodes.
2. **OD** [12]: OD introduces graph auto-encoder and filter out nodes with high reconstruction loss to remove those triggers that are outliers compared to clean ones.

We include a strong baseline that also aims to learn a clean model from the poisoned data:

1. **ABL** [13]: ABL exploits two key weaknesses of backdoor attacks: 1) models learn backdoored data much faster than clean data, with stronger attacks causing faster convergence; 2) the backdoor task is tied to a specific class. Thus, they propose a local gradient ascent (LGA) technique to trap the loss value of each example around a certain threshold. They also propose a global gradient ascent (GGA) loss function to unlearn the backdoor with a small subset of backdoor examples while continuing to learn from the remaining clean examples.

As backdoor attack is a subset of a poisoning attack, we also include three representative robust GNNs:

1. **RS** [16]: Randomized smoothing on graphs was first proposed to counter adversarial structural perturbations. We adopt this method and set the drop ratio $\beta > 0.5$ to balance the defense performance and clean accuracy. To further ensure clean accuracy, we introduce an adversarial training strategy during the training phase.
2. **GNNGuard** [14]: GNNGuard is a robust defense method for GNNs that protects against adversarial attacks by leveraging node similarity to filter out adversarial edges. It employs a multi-stages defense strategy that dynamically adjusts edge weights during training, enhancing the model’s resilience to structural perturbations.
3. **RobustGCN** [15]: RobustGCN enhances the robustness of GCN against adversarial attacks by using Gaussian distributions as node representations, which absorb the effects of adversarial changes. It also introduces a variance-based attention mechanism that assigns different weights to node neighborhoods based on their variances, reducing the propagation of adversarial effects through the graph.

G.4 Implementation Details

We test our RIGBD using different graph neural network backbones, i.e. GCN, GAT, and GraphSage. All hyperparameters of all methods are tuned based on the validation set for fair comparison. All models are trained on an A6000 GPU with 48G memory.

Table 6: Comparison of Clean Accuracy between GCN and RIGBD trained on clean graph.

Dataset	GCN	RIGBD
Cora	84.44	84.07
PubMed	85.13	85.05
OGB-arxiv	66.13	65.53

Table 7: Additional results of backdoor defense.

Attacks	Defense	Cora		PubMed		OGB-arxiv	
		ASR(%) ↓	ACC(%) ↑	ASR(%) ↓	ACC(%) ↑	ASR(%) ↓	ACC(%) ↑
GTA	GAT	76.97	84.44	89.77	82.60	OOM	OOM
	GraphSage	100.00	81.11	99.94	84.88	93.67	67.81
	RS-0.7	45.02	66.67	33.20	85.24	33.12	56.93
	RS-0.8	34.32	65.56	24.65	85.13	25.72	55.05
	RIGBD-GAT	0.02	85.19	0.08	83.66	OOM	OOM
	RIGBD-GraphSage	0.18	81.52	0.00	85.84	0.09	67.18
UGBA	GAT	100	85.19	100.00	83.05	OOM	OOM
	GraphSage	97.33	84.07	99.08	85.24	94.69	68.25
	RS-0.7	46.86	69.63	37.74	85.34	29.74	57.33
	RS-0.8	37.64	65.19	28.20	86.35	23.14	54.77
	RIGBD-GAT	0.04	84.81	0.30	82.14	OOM	OOM
	RIGBD-GraphSage	0.44	84.07	0.02	85.74	0.06	67.75
DPGBA	GAT	91.14	83.33	93.8	83.56	OOM	OOM
	GraphSage	93.48	83.33	91.8	85.79	99.53	67.76
	RS-0.7	40.96	68.52	36.31	84.98	32.81	56.66
	RS-0.8	35.79	66.30	27.13	85.74	23.41	54.45
	RIGBD-GAT	0.04	84.44	0.01	83.31	OOM	OOM
	RIGBD-GraphSage	0.26	82.11	0.06	86.35	0.03	66.61

H Results on Clean Graph

In this section, we conduct experiments to show the clean accuracy of our RIGBD when trained on a clean graph. Specifically, we follow the experimental setup described in Sec. 5.2 and remove the backdoor triggers from the poisoned graph. Then, we train a GCN and RIGBD on this clean graph. The results are shown in Tab. 6. From the table, we observe that our RIGBD achieves comparable clean accuracy to GCN. This is because our poisoned node selection strategy, defined in Eq. (5), stops when nodes continuously show different labels compared to the node with the highest prediction variance. Since nodes with high confidence are not always from the same class in a clean graph, we rarely select nodes as poisoned nodes. This highlights the adaptability of our RIGBD, even when we do not know whether the graph is clean or poisoned.

I Additional Results of Defense Performance

In this section, we provide additional results on defense performance. Specifically, we implement RIGBD with GAT and GraphSage as backbones. We also include randomized smoothing (RS) with drop ratios $\beta = 0.7$ and $\beta = 0.8$. All other settings are the same as Sec. 5.2. The results are shown in Table 7. From the table, we observe the following: **(i)** With the increase in drop ratio, randomized smoothing can degrade the ASR. However, the clean accuracy is not guaranteed. This demonstrates the superiority of our framework in degrading ASR while maintaining clean accuracy. **(ii)** Our RIGBD consistently achieves low ASR while maintaining comparable or slightly better clean accuracy compared to vanilla GNNs on all datasets. This demonstrates the flexibility and effectiveness of our framework with different backbones.

J Additional Results of the Ability to Detect Poisoned Nodes

In this section, we provide additional results of the ability to detect poisoned nodes on Cora and PubMed dataset. We present the recall and precision of RIGBD in identifying poisoned nodes. We use the same setting as in Sec. 5.2. The results are shown in Table 3. We also present the corresponding ASR and ACC to illustrate the correlation between detection ability and defense performance. Clean accuracy (Clean ACC), obtained from a model trained on the clean graph, is provided as a reference to evaluate the model’s performance on clean nodes. From the table, we observe the following:

Table 8: Results for the ability to detect poisoned nodes.

Datasets	Attacks	Clean ACC	ASR	ACC	Recall	Precision
Cora	GTA	83.5	0.00	83.70	91.2	94.0
	UGBA	83.5	0.01	84.81	96.8	100.0
	DPGBA	83.5	0.01	85.19	100.0	100.0
PubMed	GTA	84.9	0.01	84.32	82.0	90.5
	UGBA	84.9	0.01	85.13	88.7	96.6
	DPGBA	84.9	0.01	84.32	85.0	91.0
OGB-arxiv	GTA	65.8	0.01	66.51	84.9	90.3
	UGBA	65.8	0.01	65.21	95.6	96.3
	DPGBA	65.8	0.00	65.24	90.5	93.9

(i) Our RIGBD demonstrates consistently high precision, always over 90%, in detecting poisoned nodes across three attack methods in all datasets, with detection recall always exceeding 80%. This indicates that our strategy of random edge dropping with graph convolution operation defined in Eq. (3) typically leads to higher prediction variance for poisoned nodes. (ii) Although the recall for some attack methods and datasets is less than 90%, we still achieve an ASR close to 0% while maintaining ACC. This demonstrates the stability of our strategy to train a robust node classifier using Eq. (6). Even when some of the poisoned nodes are not identified, it still efficiently helps the model unlearn the triggers.

K Additional Results of Hyperparameter Analysis

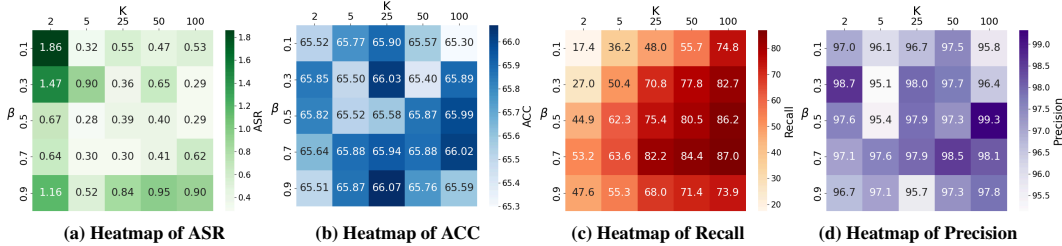


Figure 9: Hyperparameter Sensitivity Analysis

In this section, we provide additional results on how different drop ratios (β) and different numbers of iterations of random edge dropping (K) impact the ACC of RIGBD. ASR, Recall, and Precision are also provided as references. Specifically, we vary the values of K as $\{2, 5, 25, 50, 100\}$, and the values of β as $\{0.1, 0.3, 0.5, 0.7, 0.9\}$. The attack method used is DPGBA. The other settings are the same as the evaluation protocol in Sec. 5.1. The results are shown in Fig. 9. From the figure, we make the following observations: (i) Our RIGBD is stable in terms of ASR, ACC, and Precision. Notably, when the drop ratio $\beta = 0.1$ and we only conduct two iterations of random edge dropping, the recall of our poison node detection is around 17.4%. However, we still achieve robust defense performance with ASR close to 0%. This demonstrates that our robust training strategy is effective even with a lower recall. As our framework identifies the most efficient triggers that lead to large prediction variance and focuses on minimizing their impact. By doing so, the influence of less efficient triggers is inherently counteracted. In contrast, when we simply remove those 17.4% triggers from the dataset and train a model on the remaining dataset, the ASR is around 80%. (ii) As K increases, the recall also increases, empirically verifying our Theorem 1 that in expectation, the clean nodes will have stable node representations and thus stable predictions when using the graph convolution operation designed in Eq. (3). As β increases from 0.1 to 0.7, the recall also increases without a decrease in precision, demonstrating the stability of our method. When $\beta = 0.9$, only about 10% of edges remain in each iteration. Though the recall decreases slightly, we still achieve consistently high precision. This further indicates the robustness of our model against various chosen hyperparameters.

L Additional Results of Ablation Studies

In this section, we provide additional results on ablation studies on OGB-arxiv dataset to investigate the impact of random edge dropping on poison node detection and evaluate the efficacy of our robust training strategy as described in Eq. (6). Following Sec. 5.4, to evaluate the effectiveness of random edge dropping, we replace it with an intuitive method of dropping edges individually, as described in

Section 3.2, and obtain a variant named as RIGBD\E. To demonstrate the effectiveness of our robust training strategy, we implement a variant of our model, named RIGBD\R, which simply removes identified candidate poisoned nodes from the dataset. The attack method used is DPGBA. We also implement a variant called RIGBD\RE, which involves individually dropping each edge and eliminate candidate poisoned nodes. The number of iterations for random edge dropping is set to $K = 20$, with a drop ratio of $\beta = 0.5$. We report the ASR and ACC in Fig. 10. The results on scenarios where a backdoor trigger (subgraph) is linked to a poisoned node by two edges are also provided as a reference. From the figure, we observe: **(i)** In Fig. 10 (a), RIGBD\E and RIGBD\RE achieve comparable and slightly better defense performance than RIGBD\R and RIGBD\RE. However, in Fig. 10 (b), RIGBD\E and RIGBD\RE fail to degrade the ASR. This demonstrate that although drop edge individually may demonstrate comparable performance in detecting poison nodes when there is only one edge linking a trigger to a target node, it fails to defend effectively against attacks involving two edges linking a backdoor trigger to a target node. In such cases, the intuitive method of dropping each edge individually proves inadequate. **(ii)** In both settings, RIGBD\ achieve better defense performance than RIGBD\R. This demonstrates the effectiveness of our robust training strategy in handling cases where some poisoned nodes are not identified.

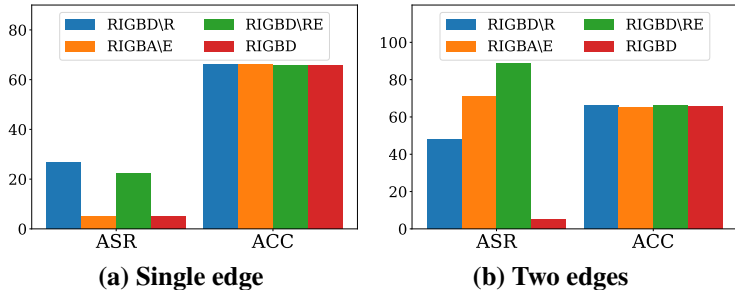


Figure 10: Ablation study on OGB-arxiv

M Additional Results of Defense Performance and Ability to Detect Poison Nodes with Different Numbers of Triggers

Table 9: Results for defense and poisoned node detection with different numbers of triggers.

Datasets	Triggers	ASR	Clean ACC	ASR	ACC	Recall	Precision
Cora	10	87.82	84.81	0.05	85.56	90.0	90.0
	20	92.62	84.44	0.00	85.19	95.0	100.0
	40	93.48	83.70	0.02	85.93	97.0	97.0
	80	96.52	82.22	0.10	84.81	94.0	98.4
	160	99.13	80.00	0.10	84.07	97.1	95.8
PubMed	20	90.73	84.88	0.01	85.21	85.0	85.0
	80	94.32	84.68	0.01	84.56	75.5	90.2
	160	96.10	84.17	0.02	84.47	82.0	90.5
	240	97.46	84.14	0.01	84.16	66.2	95.8
	320	98.07	83.77	0.02	84.04	83.0	88.2

In this section, we conduct experiments to demonstrate how varying numbers of backdoor triggers impact the performance of RIGBD in terms of backdoor defense and poisoned node detection. Specifically, we set the number of triggers to $\{10, 20, 40, 80, 160\}$ for Cora and $\{20, 80, 160, 240, 320\}$ for PubMed. The attack method used is DPGBA. The drop ratio $\beta = 0.5$, and the number of iterations for random edge dropping are set as $K = 10$ for Cora and $K = 20$ for PubMed. The results are shown in Table 9. From the table, we observe: **(i)** Though there are fluctuations in the recall and precision in detecting poisoned nodes, the precision always exceeds 85%. This indicates that our method of random edge dropping consistently leads to higher prediction variance, helping us precisely identify poisoned nodes regardless of the number of triggers. **(ii)** With the different number of triggers, our method demonstrate consistently superior performance in defense, with ASR close to 0% and ACC comparable to Clean ACC. Notably, when the number of triggers is 240 for PubMed, the detection

recall is around 66%, but we still achieve good results in terms of ASR and ACC. This further indicates the stability of our method in training a robust node classifier using Eq. (6), even if some poisoned nodes are not identified. Additional results on the visualization of prediction variance for poisoned nodes and clean nodes with different numbers of triggers are provided in Fig. 11 and Fig. 12.

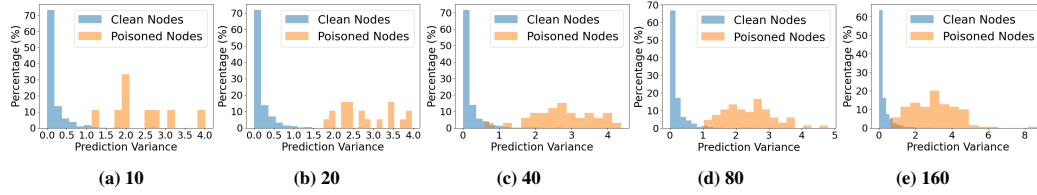


Figure 11: Visualization of prediction variance on Cora dataset with different number of triggers

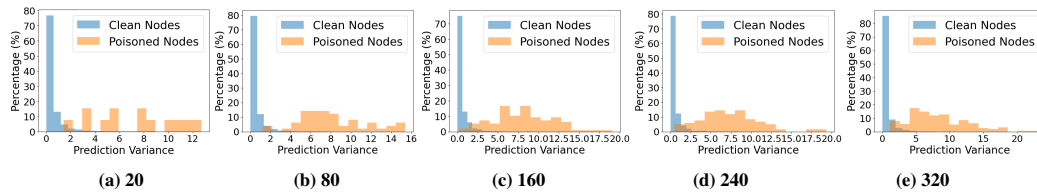


Figure 12: Visualization of prediction variance on PubMed dataset with different number of triggers